# Potential ~~U~~underestimation of ambient brown carbon absorption based on the methanol extraction method and its impacts on source analysis

Zhenqi Xu[a], Wei Feng[a], Yicheng Wang[a], Haoran Ye[a], Yuhang Wang[b], Hong Liao[a], Mingjie Xie[a,*]

[a]Collaborative Innovation Center of Atmospheric Environment and Equipment Technology, Jiangsu Key Laboratory of Atmospheric Environment Monitoring and Pollution Control, School of Environmental Science and Engineering, Nanjing University of Information Science & Technology, 219 Ningliu Road, Nanjing 210044, China

[b]School of Earth and Atmospheric Sciences, Georgia Institute of Technology, Atlanta, GA 30332, United States

*Corresponding to:

Mingjie Xie (mingjie.xie@nuist.edu.cn, mingjie.xie@colorado.edu);

Mailing address: 219 Ningliu Road, Nanjing, Jiangsu, 210044, China

**Abstract**

The methanol extraction method was widely applied to isolate organic carbon (OC) from ambient aerosols, followed by measurements of brown carbon (BrC) absorption. However, undissolved OC fractions will lead to underestimated BrC absorption. In this work, water, methanol (MeOH), MeOH/dichloromethane (MeOH/DCM, 1:1, v/v), MeOH/DCM (1:2, v/v), tetrahydrofuran (THF), and N,N-dimethylformamide (DMF) were tested for extraction efficiencies of ambient OC, and the light absorption of individual solvent extracts was determined. Among the five solvents and solvent mixtures, DMF dissolved the highest fractions of ambient OC (up to ~95%), followed by MeOH and MeOH/DCM mixtures (< 90%), and the DMF extracts had significant ($p < 0.05$) higher light absorption than other solvent extracts. This is because the OC fractions evaporating at higher temperatures (> 280°C) are less soluble in MeOH (~80%) than in DMF (~90%) and contain stronger light-absorbing chromophores. Moreover, the light absorption of DMF and MeOH extracts of collocated aerosol samples in Nanjing showed consistent temporal variations in winter when biomass burning dominated BrC absorption. While the average light absorption of DMF extracts was more than two times greater than the MeOH extracts in late spring and summer.~~distinct time series.~~ The average light absorption coefficient at 365 nm of DMF extracts was 30.7% higher ($p < 0.01$) than that of MeOH extracts. Source apportionment results indicated that the MeOH solubility of BrC associated with biomass burning, lubricating oil combustion, and coal combustion is similar to their DMF solubility. The BrC linked with unburned fossil fuels and polymerization processes of aerosol organics was less soluble in MeOH than in DMF, which was likely the main reason for the large difference in time series between MeOH and DMF extract absorption. These results highlight the

设置了格式: 字体: 小四

设置了格式: 字体: 倾斜

设置了格式: 字体: 小四

importance of testing different solvents to investigate the structures and light absorption of BrC, particularly for the low-volatility fraction potentially originating from non-combustion sources~~the MeOH insoluble OC mainly came from unburned fossil fuels and polymerization processes of aerosol organics. These results highlight the necessity of replacing MeOH with DMF for further investigations on structures and light absorption of low-volatile BrC~~.

设置了格式: 字体: 小四

设置了格式: 字体: 小四

## 1 Introduction

Besides black carbon (BC) and mineral dust, growing evidence shows that organic carbon (OC) aerosols derived from various combustion sources (e.g., biofuel and fossil fuel) and secondary processes (e.g., gas-phase oxidation, aqueous and in-cloud processes) can absorb sunlight at short visible and UV wavelengths (Laskin et al., 2015; Hems et al., 2021). The radiative forcing (RF) of the light-absorbing organic carbon, also termed "brown carbon" (BrC), is not well quantified due to the lack of its emission data, complex secondary formations, and large uncertainties in *in situ* BrC measurements (Wang et al., 2014; Wang et al., 2018; Saleh, 2020). The imaginary part of the refractive index ($k$) of BrC is required when modeling its influence on aerosols direct RF, and is retrieved by the optical closure method combing online monitoring of aerosol absorption and size distributions with Mie theory calculations (Lack et al., 2012; Saleh et al., 2013; Saleh et al., 2014). However, several pre-assumptions must be made

on aerosol morphology (spherical Mie model) and mixing states of BC and organic aerosols (OA), which might introduce large uncertainties in the estimation of $k$ (Mack et al., 2010; Xu et al., 2021).

To improve the understanding on chemical composition and light-absorbing properties of BrC chromophores, organic matter (OM) in aerosols was isolated through solvent extraction using water and/or methanol, followed by filtration and a series of instrumental analysis (e.g., UV/Vis spectrometer, liquid chromatograph-mass spectrometer; Chen and Bond, 2010; Liu et al., 2013; Lin et al., 2016). Referring to existing studies, a larger fraction of the methanol extract absorption comes from water-insoluble OM containing conjugated structures (Chen and Bond, 2010; Huang et al., 2020); the light absorption of biomass burning OM is majorly contributed by large molecules (MW > 500~1000 Da; Di Lorenzo and Young, 2016; Di Lorenzo et al., 2017) and depends on burn conditions (Saleh et al., 2014); polycyclic aromatic hydrocarbons (PAHs) and nitroaromatic compounds (NACs) are ubiquitous BrC chromophores in the atmosphere (Huang et al., 2018; Wang et al., 2019), but the identified species only explain a few percentages (< 10%) of total BrC absorption (Huang et al., 2018; Li et al., 2020).

Methanol can extract > 90% OM from biomass burning (Chen and Bond, 2010; Xie et al., 2017b), while the extraction efficiency (η, %) decreases to ~80% for ambient organic aerosols (Xie et al., 2019b; Xie et al., 2022) possibly due to other sources emitting large hydrophobic molecules and oligomerizations of small molecules during the aging process (Cheng et al., 2021; Li et al., 2021). The light-absorbing properties and structures of methanol-insoluble OC (MIOC) are still unknown. By comparing BrC characterization results of offline and online methods, some studies conclude that the MIOC dominates BrC absorption in source and ambient aerosols (Bai et al., 2020; Atwi

et al., 2022). However, the online-retrieval and offline-extraction methods are designed based on different instrumentation and purposes, and the online method depends largely on presumed and uncertain optical properties of BC (Wang et al., 2014). Given that the solvent extract absorption is not converted to particulate absorption with Mie calculations, solvent and pH effects are not accounted for, and BrC is not completely dissolved in typical solvents (e.g., water and methanol), BrC absorption in particles and solution can hardly be compared directly~~Thus, BrC absorption in particles and solution can hardly be compared directly~~. To reveal the absorption and composition of MIOC, it is necessary to find a new solvent or develop a new methodology to improve OC extraction efficiency (Shetty et al., 2019).

In this work, a series of single solvents and solvent blends were tested for extraction efficiencies of OC in ambient particulate matter with aerodynamic diameter < 2.5 μm ($PM_{2.5}$), and the sample extract absorption of each solvent was compared. The solvent or solvent mixture with the highest η value was applied to extract a matrix of collocated $PM_{2.5}$ samples followed by light absorption measurements. In our previous work, the light absorption of methanol extracts of the same samples was measured, and source apportionment was performed using organic molecular marker data (Xie et al., 2022). By comparing with the study results in Xie et al. (2022), this study evaluated ~~the~~ potential underestimation of BrC absorption in methanol and its impacts on BrC source attributions. These results suggest that different solvents should be used~~methanol should be replaced~~ in future ~~solvent extraction based~~ investigations on the absorption, composition, sources, and formation pathways of low-volatility~~e~~ BrC.

## 2. Methods

### *2.1 Solvent selection*

Five solvents and solvent mixtures including water, methanol (MeOH),

设置了格式: 字体: 小四

设置了格式: 字体: 小四

设置了格式: 字体: 小四

MeOH/dichloromethane (MeOH/DCM, 1:1, v:v), MeOH/DCM (1:2, v:v), tetrahydrofuran (THF), and N,N-dimethylformamide (DMF) were selected to extract OC from identical $PM_{2.5}$ samples to determine which solvent or solvent mixture has the highest η value. Water and methanol are the most commonly used solvents to extract BrC from source or ambient particles. Cheng et al. (2021) found that OC produced through the combustion of toluene, isooctane, and cyclohexane were more soluble in DCM than MeOH. Since a major part of BrC absorption is coming from unknown large molecules (Di Lorenzo and Young, 2016; Di Lorenzo et al., 2017), polar aprotic solvents THF and DMF were tested due to their high capacity for dissolving large polymers. Except for water and MeOH, DCM and THF were rarely used to extract OC for light absorption measurements (Cheng et al., 2021; Moschos et al. 2021), and DMF has not ever been tested for extracting BrC in literature. ~~MeOH/DCM mixtures, THF, and DMF were rarely used to extract OC for light absorption measurements~~.

设置了格式: 字体: 小四

设置了格式: 字体: 小四

设置了格式: 字体: 小四

设置了格式: 字体: 小四

*2.2 Sampling*

**Sampling for solvent test.** To compare OC extraction efficiencies and extract absorption of the five selected solvents and solvent mixtures, twenty-one ambient $PM_{2.5}$ samples were collected on the rooftop of a seven-story library building in Nanjing University of Information Science and Technology (NUIST, 32.21°N, 118.71°E). Details of the sampling site and equipment were provided by Yang et al. (2021). Two identical mid-volume samplers (Sampler I and II; $PM_{2.5}$-PUF-300, Mingye Environmental, China) equipped with 2.5 μm cut-point impactors were used for ambient air sampling during day-time (8:00 a.m.–7:00 p.m.) and night-time (8:00 p.m.–7:00 a.m. the next day), respectively, in December 2019. After the impactor, $PM_{2.5}$ in the air stream was collected on a pre-baked (550 ℃, 4 h) quartz filter (20.3 cm ×12.6 cm, Munktell Filter AB, Sweden) at a flow rate of 300 L $min^{-1}$. $PM_{2.5}$ filter and field

blank samples were sealed and stored at –20 ℃ before chemical analysis. Information about $PM_{2.5}$ samples for the solvent test is provided in Table S1 of supplementary information.

**Ambient sampling for BrC analysis.** Details of the ambient sampling were described in previous work (Qin et al., 2021; Yang et al., 2021; Xie et al., 2022). Briefly, Sampler I and II were equipped with two quartz filters in series (quartz behind quartz, QBQ method; $Q_f$ and $Q_b$) followed by adsorbents. Collocated filter and adsorbent samples were collected every sixth day during daytime and nighttime from 2018/09/28 to 2019/09/28. Field blank sampling was performed every $10^{th}$ sample to address contamination. $Q_f$ samples loaded with $PM_{2.5}$ were speciated and extracted for light absorption measurements. The OC adsorbed on $Q_b$ and its light absorption were analyzed to determine positive sampling artifacts. The adsorbents in sampler I [a polyurethane foam (PUF)/XAD-4 resin/PUF sandwich] and II (a PUF plug) were used to collect gas-phase nonpolar and polar organic compounds, respectively. The measurement results of gas- and particle-phase organic compounds were provided by Gou et al. (2021) and Qin et al. (2021).

设置了格式: 字体: 小四

*2.3 Solvent test for light absorption and extraction efficiency*

An aliquot (~6 $cm^2$) of each filter sample was extracted ultrasonically in 10 mL of each solvent or solvent mixture (HPLC grade) for 30 min (one-time extraction procedure, $N$ = 11; Table S1). After filtration, the light absorbance ($A_\lambda$) of individual solvent extracts was measured over 200–900 nm using a UV/Vis spectrometer (UV-1900, Shimadzu Corporation, Japan), and was converted to light absorption coefficient ($Abs_\lambda$, $Mm^{-1}$) by

$$Abs_\lambda = (A_\lambda - A_{700}) \times \frac{V_l}{V_a \times L} \ln(10) \qquad (1)$$

where $A_{700}$ is subtracted to correct baseline drift, $V_l$ ($m^3$) is the air volume of the extracted sample, $L$ (0.01 m) is the optical path length, and ln (10) was multiplied to transform $Abs_\lambda$ from a common to a natural logarithm (Hecobian et al., 2010). To understand if multiple extractions could draw out more BrC, a two-time extraction procedure was applied for another 10 ambient $PM_{2.5}$ samples in the same manner (Table S1). The $A_\lambda$ of the 1st and 2nd extractions (10 mL each) was measured separately for $Abs_\lambda$ calculations.

Prior to solvent extractions, the concentrations of OC and EC in each filter sample were analyzed using a thermal-optical carbon analyzer (DRI, 2001A, Atmoslytic, United States) following the IMPROVE-A protocol. OC and EC were converted to $CO_2$ step by step during two separate heating cycles [OC1 (140℃) – OC2 (280℃) – OC3 (480℃) – OC4 (580℃) in pure He, EC1 (580℃) – EC2 (740℃) – EC3 (840℃) in 98% He/2% $O_2$], and the emitted $CO_2$ during each heating step was converted to $CH_4$ and measured using a flame ionization detector (FID).

After extractions, filters extracted by MeOH, MeOH/DCM (1:1), MeOH/DCM (1:2), and THF were air-dried in a fume hood and analyzed for residual OC (rOC, μg $m^{-3}$) using the identical method. Filters extracted in water and DMF cannot be air-dried in the short term due to the low volatility of solvents, and their rOC was measured after baking at 100 ℃ for 2 h. The total amount of OC dissolved in water for each sample was also measured as water-soluble OC (WSOC) by a total organic carbon analyzer (TOC-L, Shimadzu, Japan; Yang et al., 2021). To examine if the baking process would influence rOC measurements, the rOC of filters extracted in MeOH, MeOH/DCM mixtures, and THF were also measured after the baking process and compared to those determined after air dried. The pyrolytic carbon (PC) was used to correct for sample charring and was determined when the filter transmittance or reflectance returned to its

initial value during the analysis (Schauer et al., 2003), but the formation of PC is very scarce when analyzing extracted filters. In this study, solvent-extractable OC (SEOC, μg $m^{-3}$) was determined by the difference in OC1–OC4 between pre- and post-extraction samples. The extraction efficiency (η, %) of each solvent was expressed as

$$\eta = \frac{\mathrm{SEOC}}{\mathrm{OC}} \times 100\% \quad (2)$$

Here, SEOC denotes WSOC when the solvent is water. For the ambient samples extracted twice, rOC was measured only after the two-extraction procedure was completed.

The solution mass absorption efficiency ($MAE_\lambda$, $m^2$ $g^{-1}$ C) was calculated by dividing $Abs_\lambda$ by the concentration of SEOC

$$\mathrm{MAE}_\lambda = \frac{\mathrm{Abs}_\lambda}{\mathrm{SEOC}} \quad (3)$$

and the solution absorption Ångström exponent (Å), a parameter showing the wavelength dependence of solvent extract absorption, was obtained from the regression slope of lg ($Abs_\lambda$) versus lg (λ) over 300–550 nm.

The solvent effect is not uncommon when measuring aerosol extract absorbance in difference solvents (Chen and Bond, 2010; Mo et al., 2017; Moschos et al., 2021), but is rarely accounted for in previous studies. To evaluate the influence of solvent effects on light absorption of different solvent extracts of the same sample, solutions of 4-nitrophenol at 1.90 mg $L^{-1}$, 4-nitrocatechol at 1.84 mg $L^{-1}$, and 25-PAH mixtures (Table S2) at 0.0080 mg $L^{-1}$ and 0.024 mg $L^{-1}$ (each species) in the five solvents and solvent mixtures were made up for five times and analyzed for UV/Vis spectra. The absorbance of PAH mixtures in water was not provided due to their low solubility.

设置了格式: 字体: 小四

*2.3 Measurements and analysis of ambient BrC absorption*

Collocated $Q_f$ and $Q_b$ samples were extracted using the solvent with the highest η

value once followed by light absorbance measurement. OC concentrations in $Q_f$ and $Q_b$ samples were obtained from Yang et al. (2021), and SEOC values were estimated from OC concentrations and the average η value determined in *section 2.1* for one-time extraction. In this work, $Q_b$ measurements were used to correct $Abs_\lambda$, $MAE_\lambda$, and Å of BrC in ambient $PM_{2.5}$ in the same manner as those for water and methanol extracts in Xie et al. (2022)

$$\text{Artifact-corrected Abs}_\lambda = \text{Abs}_\lambda^{Qf} - \text{Abs}_\lambda^{Qb} \quad (4)$$

$$\text{Artifact-corrected MAE}_\lambda = \frac{\text{Abs}_\lambda^{Qf} - \text{Abs}_\lambda^{Qb}}{\text{SEOC}_{Qf} - \text{OC}_{Qb}} \quad (5)$$

where $Abs^{Qf}{}_\lambda$ and $Abs^{Qb}{}_\lambda$ are $Abs_\lambda$ values of $Q_f$ and $Q_b$ samples, respectively; $SEOC_{Qf}$ represents SEOC concentrations in $Q_f$ samples; $OC_{Qb}$ denotes OC concentrations in $Q_b$ samples, assuming that OC in $Q_b$ is completely dissolved (Xie et al., 2022). Artifact corrected Å were generated from the regression slope of lg ($Abs^{Qf}{}_\lambda$ - $Abs^{Qb}{}_\lambda$) versus lg (λ) over 300 – 550 nm. Artifact-corrected $Abs_\lambda$, $MAE_\lambda$, and Å during each sampling interval were determined by averaging each pair of collocated measurements. If one of the two numbers in a pair is missed, the other number will be directly used for the specific sampling interval. To compare with previous studies based on water and/or methanol extraction methods, $Abs_\lambda$ and $MAE_\lambda$ at 365 nm were shown and discussed in this work.

Pearson's correlation coefficient (*r*) was used to show how collocated measurements of BrC in ambient $PM_{2.5}$ vary together. The coefficient of divergence (COD) was calculated to indicate consistency between collocated measurements. The relative uncertainty of BrC absorption derived from duplicate data was depicted using the average relative percent difference (ARPD, %), which was used as the uncertainty fraction for BrC measurements. Calculation methods of COD and ARPD are provided

in Text S1 of supplementary information. To examine the influence of potential BrC underestimation based on the methanol extraction method on source apportionment, positive matrix factorization (PMF) version 5.0 (U.S. Environmental Protection Agency) was applied to attribute the light absorption of aerosol extracts in methanol and solvent with the highest η to sources. The total concentration data ($Q_f$ + $Q_b$ + adsorbent) of organic compounds have been used to apportion the light absorption of MeOH-soluble OC to specific sources (Xie et al., 2022), so as to avoid the impacts of gas-particle partitioning. In this work, ~~T~~the input particulate bulk components and total organic molecular marker (OMM) data for PMF analysis were obtained from Xie et al. (2022) and are summarized in Table S3. Four- to ten-factor solutions were tested to retrieve a final factor number with the most physically interpretable base-case solution. More information on input data preparation and the factor number determination are provided in supplementary information (Text S2 and Table S4).

设置了格式: 字体: 小四

## 3. Results and discussion

### *3.1 Solvent test*

#### 3.1.1 Extraction efficiency of different solvents

The concentrations of OC and EC fractions in each sample prior to solvent extractions are listed in Table S1. SEOC concentrations and extraction efficiencies of individual solvents and solvent mixtures are detailed in Table 1. Generally, DMF presented the highest extraction efficiency of total OC whenever filter samples were extracted once (89.0 ± 7.96%) or twice (95.6 ± 3.67%), followed by MeOH (one-time extraction 82.3 ± 8.68%, two-time extraction 86.6 ± 7.86%) and MeOH/DCM mixtures (~75%, ~85%). Although THF and DMF are frequently used to dissolve polymers (e.g., polystyrene) for characterization, THF had the lowest η values (64.2 ± 8.08%, 70.1 ± 8.01%) comparable to water (66.7 ± 8.58%, 69.9 ± 5.88%). Compared with one-time

extraction, the extraction efficiencies of selected solvents were improved by a few percent when filter samples were extracted twice, and η values of MeOH/DCM mixtures became closer to those of MeOH (Table 1). These results showed that solvents can reach more than 80% of their dissolving capacity with the one-time extraction, and the ambient OC in Nanjing is more soluble in MeOH than in DCM.

From OC1 to OC4, the volatility of OC fractions is expected to decrease continuously, and the molecules in OC fractions evolving at higher temperatures should be larger than those in OC1 with similar functional groups. In Table 1, MeOH and MeOH/DCM mixtures had comparable or even higher η values (82.6 ± 25.9%–97.9 ± 5.02%) of OC1 and OC2 than DMF (88.8 ± 4.98%–97.2 ± 2.12%). But OC3 and OC4 accounted for more than 60% of OC concentrations, and DMF exhibited significant ($p < 0.05$) larger η values than other solvents, indicating that DMF had stronger dissolving capacity for large organic molecules than MeOH.

Concentrations of extracted OC fractions in MeOH, MeOH/DCM mixtures, and THF based on the two methods for rOC measurements (*section 2.2*) are compared in Figures S1 and S2. The total SEOC concentrations derived from the two methods are compared in Figure S3. All the scatter data of SEOC fell along the 1:1 line with significant correlations ($r > 0.85$, $p < 0.01$). Because the measurement uncertainty of dominant species is lower than minor ones (Hyslop and White, 2008; Yang et al., 2021), the slightly greater relative difference between the two methods for extractable OC1 was likely attributed to its low concentrations (< 1 μg $m^{-3}$; Tables 1 and S1). Thus, baking extracted filters to dryness was expected to have little influence on SEOC measurements, particularly for low-~~volatile~~ volatility OC fractions (OC2-OC4).

Although water dissolves less OC than MeOH, WSOC is intensively extracted and analyzed for its composition and light absorption (Hecobian et al., 2010; Liu et al., 2013;

Washenfelder et al., 2015). WSOC can play a significant role in changing the radiative and cloud-nucleating properties of atmospheric aerosols (Hallar et al., 2013; Taylor et al., 2017). It also served as a proxy measurement for oxygenated (OOA) or secondary organic aerosols (SOA) in some regions (Kondo et al., 2007; Weber et al., 2007). In previous work, MeOH was commonly used as the most efficient solvent in extracting OC from biomass burning ($\eta$ > 90%; Chen and Bond, 2010; Xie et al., 2017b) and ambient particles ($\eta$ ~80%; Xie et al., 2019b; Xie et al., 2022). MeOH-insoluble OC has rarely been investigated through direct solvent-extraction followed by instrumental analysis. There is evidence showing that BrC absorption is associated mostly with large molecular weight and extremely low-~~volatile~~ volatility species (Saleh et al., 2014; Di Lorenzo and Young, 2016; Di Lorenzo et al., 2017). Compared with DMF, the lower capability of MeOH in dissolving OC3 and OC4 would lead to an underestimation of BrC absorption in atmospheric aerosols.

3.1.2 Light absorption of different solvent extracts

Table 2 shows the average $Abs_{\lambda}$ and $MAE_{\lambda}$ values of different solvent extracts at 365 and 550 nm. The $Abs_{\lambda}$ and $MAE_{\lambda}$ spectra of selected samples are illustrated in Figure S4. Not including DMF, MeOH extracts exhibited the strongest light absorption. Since MeOH can dissolve more OC3 and OC4 than DCM (Table 1), the $Abs_{\lambda}$ and $MAE_{\lambda}$ of MeOH/DCM extracts decreased as the fraction of DCM increased in solvent mixtures (Table 2 and Figure S4). Water and THF extracts had the smallest $Abs_{\lambda}$ and $MAE_{\lambda}$ due to their low extraction efficiencies for low-~~volatile~~ volatility OC (OC2-OC4; Table 1). In comparison to MeOH extracts, $Abs_{365/550}$ and $MAE_{365/550}$ of DMF extracts were at least more than 40% higher ($p$ < 0.05). Given that the relative difference in extraction efficiency of total OC between MeOH and DMF was less than 10% and DMF dissolved more OC3 and OC4 than other solvents (Table 1), low-~~volatile~~ volatility OC

带格式的: 不对齐到网格

should contain stronger light-absorbing chromophores (Saleh et al., 2014) and its mass fraction might determine the difference in BrC absorption across solvent extraction methods. Moreover, the relative difference in $Abs_{\lambda}$ and $MAE_{\lambda}$ between MeOH and DMF extracts increased with wavelength (Table 2 and Figure S4). This is because the light absorption of DMF extracts that contain stronger BrC chromophores depends less on wavelengths than other solvent extracts (Å ~4.5, Table 2). As shown in Figure S5, average Å and $MAE_{365/550}$ values of individual solvent extracts in Table 2 are negatively correlated.

In this work, insoluble organic particles coming off the filter during sonication might lead to overestimated SEOC concentrations and η values, and then the $MAE_{\lambda}$ of solvent extracts would be underestimated. Previous studies rarely considered the loss of insoluble OC during the extraction process (Yan et al., 2020), of which the impact on $MAE_{\lambda}$ calculation was still inconclusive. But $Abs_{\lambda}$ measurements would never be influenced, as the light absorbance of solvent extracts was analyzed after filtration. In Table 2, the second extraction only increases the average $Abs_{365}$ and $Abs_{550}$ values of DMF extracts by 6.70% ($p$ = 0.78) and 6.76% ($p$ = 0.77), respectively. We suspected that the difference in η values of DMF between one-time and two-time extraction procedures was mainly ascribed to the detachment of insoluble OC particles.

In Figure ~~S5~~S6, the absorbance spectra of 4-nitrophenol and 4-nitrocatechol in water shift toward longer wavelengths compared to their MeOH solution. This is because neutral and deprotonated forms of 4-nitrophenol and 4-nitrocatechol may have different absorbance spectra, and these two compounds are deprotonated at pH ≈ 7 (Lin et al., 2015b, 2017). The strong light absorption of 4-nitrophenol and 4-nitrocatechol in DMF at 450 nm was not observed in other solvents, and was likely caused by unknown reactions. Then the solvent effect introduced by DMF might overestimate the light

设置了格式: 字体: 小四

设置了格式: 字体: 小四

设置了格式: 字体: 小四

带格式的: 普通(网站), 两端对齐, 缩进: 首行缩进: 1.77 字符, 不对齐到网格

absorption of low-molecular-weight (LMW) nitrophenol-like species at > 400 nm in source or ambient aerosols. Evidence shows that BrC absorption is dominated by large molecules with extremely low volatility (Saleh et al., 2014; Di Lorenzo and Young, 2016; Di Lorenzo et al., 2017), and LMW nitrophenol-like species have very low contributions to particulate OM (e.g., < 1%) and aerosol extract absorption (e.g., <10%) (Mohr et al., 2013; Zhang et al., 2013; Teich et al., 2017; Xie et al., 2019a, 2020; Li et al., 2020). The shapes of the light absorption spectra of aerosol extracts in DMF were similar to other solvents (Figure S4) and PAH solutions (Figure S6g-l), and no elevation in light absorption appeared at 400–500 nm. Thus, the overestimated absorption of LMW nitrophenol-like species in DMF might not substantially impact the overall BrC absorption of aerosol extracts. ~~the UV/Vis spectra of 4-nitrophenol and 4-nitrocatechol in DMF are very different from other solvents with maximum absorbance at ~450 nm, indicating that the solvent type should influence solution absorption. However,~~Furthermore, the absorbance of 4-nitrophenol and 4-nitrocatechol in DMF at 365 nm ($A_{365}$) was lower than that in MeOH, and PAH solutions showed very similar absorbance spectra across the five solvents (Figure ~~S5g~~S6g ~~–~~l and Table ~~S4~~S5). Considering that low-~~volatile –~~volatility OC fractions (e.g., OC3 and OC4) in the ambient are less water soluble (Table 1) and have a high degree of conjugation (Chen and Bond, 2010; Lin et al., 2014), their structures are probably featured by a PAH skeleton. Therefore, the large difference in $Abs_{365}$ between DMF and MeOH extracts (Table 2) was primarily ascribed to the fact that DMF can dissolve more OC3 and OC4 than methanol (Table 1). However, we cannot rule out the impact of solvent effects on the comparison of light absorption spectra between MeOH and DMF extracts (Figure S4)~~, but not the solvent effect.~~ , and more work is warranted in identifying the structures more soluble in DMF than in MeOH.

*3.2 Collocated measurements and temporal variability*

$Abs_{365}$ values of collocated $Q_f$ and $Q_b$ extracts in DMF are summarized in Table ~~S5~~S6. No significant difference was observed ($Q_f$ $p = 0.96$; $Q_b$ $p = 0.42$) between the two samplers. After $Q_b$ corrections, $Abs_{365}$, $MAE_{365}$, and Å of DMF extractable OC ($Abs_{365,d}$, $MAE_{365,d}$, and $Å_d$) in $PM_{2.5}$ were calculated by averaging each pair of duplicate $Q_f$–$Q_b$ data, and are compared with those of methanol extracts ($Abs_{365,m}$, $MAE_{365,m}$, and $Å_m$) in Table 3. Figure 1 shows comparisons between collocated measurements of $Abs_{365,d}$, $MAE_{365,d}$, and $Å_d$. Generally, all comparisons indicated good agreement with COD < 0.20 (0.094–0.15). $Abs_{365,d}$ and $MAE_{365,d}$ had comparable uncertainty fractions (ARPD, 22.7% and 24.5%, Figure 1) as $Abs_{365,m}$ and $MAE_{365,m}$ (28.4% and 28.8%; Xie et al., 2022). Since different primary combustion sources can have similar spectral dependence for BrC absorption (Chen and Bond, 2010; Xie et al., 2017b; Xie et al., 2018; Xie et al., 2019a), most $Å_d$ data clustered on the identity line with much lower variability than $Abs_{365,d}$ and $MAE_{365,d}$. As shown in Table 3, average $Abs_{365,d}$ and $MAE_{365,d}$ values were 30.7% ($p < 0.01$) and 17.3% ($p < 0.05$) larger than average $Abs_{365,m}$ and $MAE_{365,m}$. Because the $k$ value of BrC in bulk solution is directly estimated from $Abs_\lambda$ or $MAE_\lambda$ (Liu et al., 2013; Liu et al., 2016; Lu et al., 2015), the estimation method needs to be revised when ambient BrC is extracted using DMF instead of MeOH. Both $MAE_{365,d}$ and $MAE_{365,m}$ were negatively correlated ($p < 0.01$) with their corresponding Å values (Figure S7), and ~~In comparison to $Å_m$ (6.81± 1.64; Table 3),~~ the lower average $Å_d$ (5.25 ± 0.64, $p < 0.01$) compared to $Å_m$ (6.81± 1.64; Table 3) supports that more-absorbing BrC had less spectral dependence than less-absorbing BrC.

Figure 2 compares the time series of $Abs_{365}$, $MAE_{365}$, and Å between the DMF and MeOH extracts. Both DMF and MeOH extracts had significant ($p < 0.05$) higher

设置了格式: 字体: 小四
设置了格式: 字体: 小四
设置了格式: 字体: 小四
设置了格式: 字体: 小四
设置了格式: 字体: 小四

absorption at night-time than during the daytime due to the “photo-bleaching” effect (Zhang et al., 2020; Xie et al., 2022). All the three parameters of DMF and MeOH extracts exhibited consistency in winter (Figure 2) when biomass burning dominated BrC absorption (Xie et al., 2022). While in later spring and summer (2019/05/15–2019/08/01), average $Abs_{365,d}$ and $MAE_{365,d}$ values were more than two times greater than the average $Abs_{365,m}$ and $MAE_{365,m}$. Many studies have identified a temporal pattern of BrC absorption with winter maxima and summer minima based on water/MeOH extraction methods (Lukács et al., 2007; Zhang et al., 2010; Du et al., 2014; Zhu et al., 2018). Due to the low capability of water and MeOH in dissolving large BrC molecules, BrC absorption and its temporal variations in these studies might be biased. Moreover, the identification of BrC sources using receptor models is highly dependent on the difference in the time series of input species (Dall'Osto et al., 2013). Then, using DMF instead of MeOH for BrC extraction and measurements will lead to distinct source apportionment results.

*3.3 Sources of DMF and MeOH Extractable BrC*

A final factor number of eight was determined based on the interpretability of different base-case solutions (four to ten factors), the change in $Q/Q_{exp}$ with factor numbers, and robustness analysis (Text S2 and Table S4). Normalized factor profiles of seven- to nine-factor solutions are compared in Figure ~~S6~~S8. The seven-factor solution failed to resolve the lubricating oil combustion factor characterized by hopanes and steranes (Figure ~~S6c~~S8c). An unknown factor containing various source tracers related to crustal dust ($Ca^{2+}$ and $Mg^{2+}$), lubricating oil (hopanes and steranes), and soil microbiota (sugar and sugar alcohols) was identified in the nine-factor solution (Figure ~~S6i~~S8i). Median and mean values of input $Abs_{365,d}$, $Abs_{365,}$~~$_m$~~$_m$, and bulk component concentrations agreed well with PMF estimations (Table ~~S6~~S7), and the strong

设置了格式: 字体: 小四

correlations ($r$ = 0.86–0.99) between observations and PMF estimations indicated that the eight-factor solution simulated the time series of input species well. In comparison to Xie et al. (2022), where $Abs_{365}$ of MeOH and water extracts were apportioned to nine sources using the same speciation data, this work lumped secondary nitrate and sulfate to the same factor (termed "secondary inorganics", Figure ~~S6h~~S8h), and the other seven factors had similar factor profiles linked with biomass burning, non-combustion fossil, lubricating oil combustion, coal combustion, dust resuspension, biogenic emission, and isoprene oxidation. Interpretations of individual factors based on characteristic source tracers and contribution time series were provided in previous work (Gou et al., 2021; Xie et al., 2022).

The average relative contributions of the identified factors to $Abs_{365,d}$, $Abs_{365,m}$, and bulk components are listed in Table ~~S7~~S8. Consistent contribution distributions of $Abs_{365,m}$ were observed between Xie et al. (2022) and this study, indicating that the PMF results were robust to the inclusion of $Abs_{365,d}$ data. Figure 3 compares the time series of factor contributions to $Abs_{365,d}$ and $Abs_{365,m}$. ARPD and COD values between factor contributions to $Abs_{365,d}$ and $Abs_{365,m}$ and the absolute difference are exhibited in Figure S9.~~,~~ ~~Although~~ $Abs_{365,d}$ and $Abs_{365,m}$ had comparable contributions from biomass burning, lubricating oil combustion, and coal combustion (Figure 3a, c, d~~),~~). The small COD values of these three factors (0.0041–0.17) indicated no significant divergence. The biogenic emission and isoprene oxidation factors exhibited complete difference (ARPD = 200%, COD = 1; Figure S9f, g) as they had no contribution to $Abs_{365,m}$. Among the eight factors, the non-combustion fossil, dust resuspension, and isoprene oxidation factors had the largest median difference in factor contributions to $Abs_{365,d}$ and $Abs_{365,m}$ (0.63–0.67 $Mm^{-1}$) with substantial heterogeneity (COD > 0.20), followed by the secondary inorganics factor (0.20 $Mm^{-1}$, COD = 0.41). The temporal

设置了格式: 上标

variations of the absolute difference shown in Figure S9 are identical to the contributions of individual factors to $Abs_{365,d}$ or $Abs_{365,m}$ (Figure 3). ~~other sources had significant ($p < 0.01$) higher average contributions to $Abs_{365,d}$ than $Abs_{365,m}$.~~

The non-combustion fossil factor represents unburned fossil-fuel emissions (e.g., petroleum products), which contain substantial large organic molecules (e.g., high MW PAHs; Simoneit and Fetzer, 1996; Mi et al., 2000). This might explain why the non-combustion fossil factor contributed more $Abs_{365,d}$ than $Abs_{365,m}$ all over the year (Figure S9b). Dust resuspension and isoprene oxidation factors show prominent contributions to $Abs_{365,d}$ in spring and summer, respectively (Figure 3e, g). The dust resuspension factor had the highest average contributions to both crustal materials ($Ca^{2+}$ and $Mg^{2+}$) and carbonaceous species (OC and EC; Table ~~S7~~ S8 and Figure ~~S6~~S8), and was considered a mixed source of crustal dust and motor vehicle emissions (Yu et al., 2020; Xie et al., 2022). Besides the influences from primary emissions, aging processes of organic components in dust aerosols can induce the formation of BrC through iron-catalyzed polymerization (Link et al., 2020; Al-Abadleh, 2021; Chin et al., 2021). It was demonstrated that the isoprene-derived polymerization products through aerosol-phase reactions are light-absorbing chromophores (Lin et al., 2014; Nakayama et al., 2015). This might explain the elevated difference between $Abs_{365,d}$ and $Abs_{365,m}$ contributions of the isoprene oxidation factor in summer (Figure S9g). The biogenic emission factor was characterized by tracers related to microbiota activities (sugar and sugar alcohols) and decomposition of high plant materials (odd-numbered alkanes) in soil (Rogge et al., 1993; Simoneit et al., 2004), and had negligible contributions (< 0.1%) to $Abs_{365,d}$ and $Abs_{365,m}$. Evidence shows that secondary BrC can be generated through gas-phase reactions of anthropogenic volatile organic compounds with $NO_X$ (Nakayama et al., 2010; Liu et al., 2016; Xie et al., 2017a), aqueous reactions of SOA

with reduced nitrogen-containing species (e.g., $NH_4^+$; Updyke et al., 2012; Powelson et al., 2014; Lin et al., 2015a), and evaporation of water from droplets in the atmosphere containing soluble organics (Nguyen et al., 2012; Kasthuriarachchi et al., 2020). These processes can also lead to the formation of low-volatility oligomers (Nguyen et al., 2012; Song et al., 2013), and ~~T~~their contributions might be lumped into the secondary inorganics factor due to the lack of OMMs. According to these results, one possible explanation for the difference in time series between $Abs_{365,d}$ and $Abs_{365,m}$ (Figure 2) is that large BrC molecules from unburned fossil fuels and atmospheric processes are less soluble in MeOH than in DMF.

## 4. Conclusions and implications

~~The c~~Comparisons of extraction efficiencies and light absorption of ~~ambient OC~~ ambient aerosol extracts across selected solvents and solvent mixtures ~~reveal~~ indicate that ~~the necessity of replacing~~ MeOH may sometimes be replaced with DMF for measuring BrC absorption ~~in ambient aerosols~~, as low-~~volatile~~ volatility OC fractions containing strong chromophores are less soluble in MeOH than in DMF. ~~The light absorption measurements of different solvent extracts show that DMF can extract more light absorbing materials from ambient aerosols than MeOH.~~ Existing modeling studies on the radiative forcing of BrC (Feng et al., 2013; Wang et al., 2014; Zhang et al., 2020) often retrieved or estimated its optical properties from laboratory or ambient measurements based on water/methanol extraction methods (Chen and Bond, 2010; Hecobian et al., 2010; Liu et al., 2013; Zhang et al., 2013), and had a potential to ~~probably~~ underestimate~~d~~ the contribution of BrC to total aerosol absorption. However, the influence of the solvent effect was not accounted for in this work when comparing the light absorption of different solvent extracts. The difference between MeOH and DMF extract absorption might change with the time and location due to the variations

设置了格式: 字体: 小四

设置了格式: 字体: 小四

in BrC sources. The results of this work also imply the necessity of applying different solvents or combinations of solvents with broad polarity and dissolving capability to study BrC composition and absorption, particularly for low-volatility fractions.

Although light-absorbing properties of DMF and MeOH extracts had good agreement in cold periods, when biomass and coal burning sources dominated BrC emissions, their distinct time series in spring and summer implies that the contributions of certain BrC sources were underestimated or missed when the MeOH extraction method was used. Source apportionment results of $Abs_{365,d}$ and $Abs_{365,m}$ based on organic molecular marker data indicated that large and methanol insoluble BrC molecules are likely coming from unburned fossil fuels and polymerization of aerosol organics. Laboratory studies have observed the polymerization process through heterogeneous reactions of several precursors (e.g., catechol; Lin et al., 2014; Link et al., 2020), but the structures and light-absorbing properties of potential polymerization products in ambient aerosols (Figure 3e, g) are less understood and warrant further study.

设置了格式: 字体: 小四

设置了格式: 字体: 小四

***Data availability***

Data used in the writing of this paper is available at the Harvard Dataverse (https://doi.org/10.7910/DVN/CGHPXB~~https://doi.org/10.7910/DVN/CGHPXB~~, Xu et al., 2022)

***Author contributions***

MX designed the research. ZX, WF, YW, and HY performed laboratory experiments. ZX, WF, and MX analyzed the data. ZX and MX wrote the paper with significant contributions from YW and HL.

## *Competing interests*

The authors declare that they have no conflict of interest.

## *Acknowledgments*

This work was supported by the National Natural Science Foundation of China (NSFC, 42177211, 41701551).

## References

Al-Abadleh, H. A.: Aging of atmospheric aerosols and the role of iron in catalyzing brown carbon formation, Environ. Sci.: Atmos., 1, 297-345, 10.1039/D1EA00038A, 2021.

Atwi, K., Cheng, Z., El Hajj, O., Perrie, C., and Saleh, R.: A dominant contribution to light absorption by methanol-insoluble brown carbon produced in the combustion of biomass fuels typically consumed in wildland fires in the United States, Environ. Sci.: Atmos., 10.1039/D1EA00065A, 2022.

Bai, Z., Zhang, L., Cheng, Y., Zhang, W., Mao, J., Chen, H., Li, L., Wang, L., and Chen, J.: Water/methanol-insoluble brown carbon can dominate aerosol-enhanced light absorption in port cities, Environ. Sci. Technol., 54, 14889-14898, 10.1021/acs.est.0c03844, 2020.

Chen, Y., and Bond, T. C.: Light absorption by organic carbon from wood combustion, Atmos. Chem. Phys., 10, 1773-1787, 10.5194/acp-10-1773-2010, 2010.

Cheng, Z., Atwi, K., Hajj, O. E., Ijeli, I., Fischer, D. A., Smith, G., and Saleh, R.: Discrepancies between brown carbon light-absorption properties retrieved from online and offline measurements, Aerosol Sci. Technol., 55, 92-103, 10.1080/02786826.2020.1820940, 2021.

Chin, H., Hopstock, K. S., Fleming, L. T., Nizkorodov, S. A., and Al-Abadleh, H. A.: Effect of aromatic ring substituents on the ability of catechol to produce brown carbon in iron(iii)-catalyzed reactions, Environ. Sci.: Atmos., 1, 64-78, 10.1039/D0EA00007H, 2021.

Dall'Osto, M., Querol, X., Amato, F., Karanasiou, A., Lucarelli, F., Nava, S., Calzolai, G., and Chiari, M.: Hourly elemental concentrations in PM2.5 aerosols sampled simultaneously at urban background and road site during SAPUSS – diurnal variations and PMF receptor modelling, Atmos. Chem. Phys., 13, 4375-4392, 10.5194/acp-13-4375-2013, 2013.

Di Lorenzo, R. A., and Young, C. J.: Size separation method for absorption characterization in brown carbon: Application to an aged biomass burning sample, Geophys. Res. Lett., 43, 458-465, 10.1002/2015gl066954, 2016.

Di Lorenzo, R. A., Washenfelder, R. A., Attwood, A. R., Guo, H., Xu, L., Ng, N. L., Weber, R. J., Baumann, K., Edgerton, E., and Young, C. J.: Molecular-size-separated brown carbon absorption for biomass-burning aerosol at multiple field sites, Environ. Sci. Technol., 51, 3128-3137, 10.1021/acs.est.6b06160, 2017.

Du, Z., He, K., Cheng, Y., Duan, F., Ma, Y., Liu, J., Zhang, X., Zheng, M., and Weber, R.: A yearlong study of water-soluble organic carbon in Beijing I: Sources and its primary vs. secondary nature, Atmos. Environ., 92, 514-521, https://doi.org/10.1016/j.atmosenv.2014.04.060, 2014.

Feng, Y., Ramanathan, V., and Kotamarthi, V. R.: Brown carbon: a significant atmospheric absorber of solar radiation? Atmos. Chem. Phys., 13, 8607-8621, 10.5194/acp-13-8607-2013, 2013.

Gou, Y., Qin, C., Liao, H., and Xie, M.: Measurements, gas/particle partitioning, and sources of nonpolar organic molecular markers at a suburban site in the west Yangtze River Delta, China, J. Geophys. Res. Atmos., 126, e2020JD034080, https://doi.org/10.1029/2020JD034080, 2021.

Hallar, A. G., Lowenthal, D. H., Clegg, S. L., Samburova, V., Taylor, N., Mazzoleni, L. R., Zielinska, B. K., Kristensen, T. B., Chirokova, G., McCubbin, I. B., Dodson, C., and Collins, D.: Chemical and

hygroscopic properties of aerosol organics at Storm Peak Laboratory, J. Geophys. Res. Atmos., 118, 4767-4779, https://doi.org/10.1002/jgrd.50373, 2013.
Hecobian, A., Zhang, X., Zheng, M., Frank, N., Edgerton, E. S., and Weber, R. J.: Water-Soluble Organic Aerosol material and the light-absorption characteristics of aqueous extracts measured over the Southeastern United States, Atmos. Chem. Phys., 10, 5965-5977, 10.5194/acp-10-5965-2010, 2010.
Hems, R. F., Schnitzler, E. G., Liu-Kang, C., Cappa, C. D., and Abbatt, J. P. D.: Aging of atmospheric brown carbon aerosol, ACS Earth Space Chem., 5, 722-748, 10.1021/acsearthspacechem.0c00346, 2021.
Huang, R.-J., Yang, L., Cao, J., Chen, Y., Chen, Q., Li, Y., Duan, J., Zhu, C., Dai, W., Wang, K., Lin, C., Ni, H., Corbin, J. C., Wu, Y., Zhang, R., Tie, X., Hoffmann, T., O'Dowd, C., and Dusek, U.: Brown carbon aerosol in urban Xi'an, northwest China: The composition and light absorption properties, Environ. Sci. Technol., 52, 6825-6833, 10.1021/acs.est.8b02386, 2018.
Huang, R.-J., Yang, L., Shen, J., Yuan, W., Gong, Y., Guo, J., Cao, W., Duan, J., Ni, H., Zhu, C., Dai, W., Li, Y., Chen, Y., Chen, Q., Wu, Y., Zhang, R., Dusek, U., O'Dowd, C., and Hoffmann, T.: Water-insoluble organics dominate brown carbon in wintertime urban aerosol of China: Chemical characteristics and optical properties, Environ. Sci. Technol., 54, 7836-7847, 10.1021/acs.est.0c01149, 2020.
Hyslop, N. P., and White, W. H.: An evaluation of interagency monitoring of protected visual environments (IMPROVE) collocated precision and uncertainty estimates, Atmos. Environ., 42, 2691-2705, https://doi.org/10.1016/j.atmosenv.2007.06.053, 2008.
Kasthuriarachchi, N. Y., Rivellini, L.-H., Chen, X., Li, Y. J., and Lee, A. K. Y.: Effect of relative humidity on secondary brown carbon formation in aqueous droplets, Environ. Sci. Technol., 54, 13207-13216, 10.1021/acs.est.0c01239, 2020.
Kondo, Y., Miyazaki, Y., Takegawa, N., Miyakawa, T., Weber, R. J., Jimenez, J. L., Zhang, Q., and Worsnop, D. R.: Oxygenated and water-soluble organic aerosols in Tokyo, J. Geophys. Res. Atmos., 112, D01203, 10.1029/2006jd007056, 2007.
Lack, D. A., Langridge, J. M., Bahreini, R., Cappa, C. D., Middlebrook, A. M., and Schwarz, J. P.: Brown carbon and internal mixing in biomass burning particles, Proc. Natl. Acad. Sci. U.S.A., 109, 14802-14807, 10.1073/pnas.1206575109, 2012.
Laskin, A., Laskin, J., and Nizkorodov, S. A.: Chemistry of atmospheric brown carbon, Chem. Rev., 115, 4335-4382, 10.1021/cr5006167, 2015.
Li, X., Yang, Y., Liu, S., Zhao, Q., Wang, G., and Wang, Y.: Light absorption properties of brown carbon (BrC) in autumn and winter in Beijing: Composition, formation and contribution of nitrated aromatic compounds, Atmos. Environ., 223, 117289, https://doi.org/10.1016/j.atmosenv.2020.117289, 2020.
Li, Y., Ji, Y., Zhao, J., Wang, Y., Shi, Q., Peng, J., Wang, Y., Wang, C., Zhang, F., Wang, Y., Seinfeld, J. H., and Zhang, R.: Unexpected oligomerization of small α-dicarbonyls for secondary organic aerosol and brown carbon formation, Environ. Sci. Technol., 55, 4430-4439, 10.1021/acs.est.0c08066, 2021.
Lin, P., Laskin, J., Nizkorodov, S. A., and Laskin, A.: Revealing brown carbon chromophores produced in reactions of methylglyoxal with ammonium sulfate, Environ. Sci. Technol., 49, 14257-14266, 10.1021/acs.est.5b03608, 2015a
Lin, P., Liu, J. M., Shilling, J. E., Kathmann, S. M., Laskin, J., and Laskin, A.: Molecular characterization of brown carbon (BrC) chromophores in secondary organic aerosol generated from photo-oxidation of toluene, Phys. Chem. Chem. Phys., 17, 23312-23325, 10.1039/c5cp02563j, 2015b.
Lin, P., Bluvshtein, N., Rudich, Y., Nizkorodov, S. A., Laskin, J., and Laskin, A.: Molecular chemistry of atmospheric brown carbon inferred from a nationwide biomass burning event, Environ. Sci. Technol., 51, 11561-11570, 10.1021/acs.est.7b02276, 2017.
Lin, P., Aiona, P. K., Li, Y., Shiraiwa, M., Laskin, J., Nizkorodov, S. A., and Laskin, A.: Molecular characterization of brown carbon in biomass burning aerosol particles, Environ. Sci. Technol., 50, 11815-11824, 10.1021/acs.est.6b03024, 2016.
Lin, Y.-H., Budisulistiorini, S. H., Chu, K., Siejack, R. A., Zhang, H., Riva, M., Zhang, Z., Gold, A., Kautzman, K. E., and Surratt, J. D.: Light-absorbing oligomer formation in secondary organic aerosol from reactive uptake of isoprene epoxydiols, Environ. Sci. Technol., 48, 12012-12021, 10.1021/es503142b, 2014.
Link, N., Removski, N., Yun, J., Fleming, L. T., Nizkorodov, S. A., Bertram, A. K., and Al-Abadleh, H. A.: Dust-catalyzed oxidative polymerization of catechol and its impacts on ice nucleation efficiency and optical properties, ACS Earth Space Chem., 4, 1127-1139, 10.1021/acsearthspacechem.0c00107, 2020.
Liu, J., Bergin, M., Guo, H., King, L., Kotra, N., Edgerton, E., and Weber, R. J.: Size-resolved measurements of brown carbon in water and methanol extracts and estimates of their contribution to

设置了格式: 字体颜色: 自动设置, 非突出显示
设置了格式: 字体颜色: 自动设置, 非突出显示
设置了格式: 字体颜色: 自动设置, 非突出显示
设置了格式: 字体颜色: 自动设置, 非突出显示
设置了格式: 字体颜色: 自动设置, 非突出显示
设置了格式: 字体颜色: 自动设置, 非突出显示
设置了格式: 字体颜色: 自动设置, 非突出显示
设置了格式: 字体颜色: 自动设置, 非突出显示
设置了格式: 字体颜色: 自动设置, 非突出显示
设置了格式: 字体颜色: 自动设置, 非突出显示

ambient fine-particle light absorption, Atmos. Chem. Phys., 13, 12389-12404, 10.5194/acp-13-12389-2013, 2013.
Liu, J., Lin, P., Laskin, A., Laskin, J., Kathmann, S. M., Wise, M., Caylor, R., Imholt, F., Selimovic, V., and Shilling, J. E.: Optical properties and aging of light-absorbing secondary organic aerosol, Atmos. Chem. Phys., 16, 12815-12827, 10.5194/acp-16-12815-2016, 2016.
Lu, Z., Streets, D. G., Winijkul, E., Yan, F., Chen, Y., Bond, T. C., Feng, Y., Dubey, M. K., Liu, S., Pinto, J. P., and Carmichael, G. R.: Light absorption properties and radiative effects of primary organic aerosol emissions, Environ. Sci. Technol., 49, 4868-4877, 10.1021/acs.est.5b00211, 2015.
Lukács, H., Gelencsér, A., Hammer, S., Puxbaum, H., Pio, C., Legrand, M., Kasper-Giebl, A., Handler, M., Limbeck, A., Simpson, D., and Preunkert, S.: Seasonal trends and possible sources of brown carbon based on 2-year aerosol measurements at six sites in Europe, J. Geophys. Res. Atmos., 112, https://doi.org/10.1029/2006JD008151, 2007.
Mack, L. A., Levin, E. J. T., Kreidenweis, S. M., Obrist, D., Moosmüller, H., Lewis, K. A., Arnott, W. P., McMeeking, G. R., Sullivan, A. P., Wold, C. E., Hao, W. M., Collett Jr, J. L., and Malm, W. C.: Optical closure experiments for biomass smoke aerosols, Atmos. Chem. Phys., 10, 9017-9026, 10.5194/acp-10-9017-2010, 2010.
Mo, Y., Li, J., Liu, J., Zhong, G., Cheng, Z., Tian, C., Chen, Y., and Zhang, G.: The influence of solvent and pH on determination of the light absorption properties of water-soluble brown carbon, Atmos. Environ., 161, 90-98, https://doi.org/10.1016/j.atmosenv.2017.04.037, 2017.
Mohr, C., Lopez-Hilfiker, F. D., Zotter, P., Prévôt, A. S. H., Xu, L., Ng, N. L., Herndon, S. C., Williams, L. R., Franklin, J. P., Zahniser, M. S., Worsnop, D. R., Knighton, W. B., Aiken, A. C., Gorkowski, K. J., Dubey, M. K., Allan, J. D., and Thornton, J. A.: Contribution of nitrated phenols to wood burning brown carbon light absorption in Detling, United Kingdom during winter time, Environ. Sci. Technol., 47, 6316-6324, 10.1021/es400683v, 2013.
Moschos, V., Gysel-Beer, M., Modini, R. L., Corbin, J. C., Massabò, D., Costa, C., Danelli, S. G., Vlachou, A., Daellenbach, K. R., Szidat, S., Prati, P., Prévôt, A. S. H., Baltensperger, U., and El Haddad, I.: Source-specific light absorption by carbonaceous components in the complex aerosol matrix from yearly filter-based measurements, Atmos. Chem. Phys., 21, 12809-12833, 10.5194/acp-21-12809-2021, 2021.
Mi, H.-H., Lee, W.-J., Chen, C.-B., Yang, H.-H., and Wu, S.-J.: Effect of fuel aromatic content on PAH emission from a heavy-duty diesel engine, Chemosphere, 41, 1783-1790, https://doi.org/10.1016/S0045-6535(00)00043-6, 2000.
Nakayama, T., Matsumi, Y., Sato, K., Imamura, T., Yamazaki, A., and Uchiyama, A.: Laboratory studies on optical properties of secondary organic aerosols generated during the photooxidation of toluene and the ozonolysis of α-pinene, J. Geophys. Res. Atmos., 115, D24204, 10.1029/2010jd014387, 2010.
Nakayama, T., Sato, K., Tsuge, M., Imamura, T., and Matsumi, Y.: Complex refractive index of secondary organic aerosol generated from isoprene/NOx photooxidation in the presence and absence of SO2, J. Geophys. Res. Atmos., 120, 7777-7787, https://doi.org/10.1002/2015JD023522, 2015.
Nguyen, T. B., Lee, P. B., Updyke, K. M., Bones, D. L., Laskin, J., Laskin, A., and Nizkorodov, S. A.: Formation of nitrogen- and sulfur-containing light-absorbing compounds accelerated by evaporation of water from secondary organic aerosols, J. Geophys. Res. Atmos., 117, D01207, 10.1029/2011jd016944, 2012.
Powelson, M. H., Espelien, B. M., Hawkins, L. N., Galloway, M. M., and De Haan, D. O.: Brown carbon formation by aqueous-phase carbonyl compound reactions with amines and ammonium sulfate, Environ. Sci. Technol., 48, 985-993, 10.1021/es4038325, 2014.
Qin, C., Gou, Y., Wang, Y., Mao, Y., Liao, H., Wang, Q., and Xie, M.: Gas–particle partitioning of polyol tracers at a suburban site in Nanjing, east China: increased partitioning to the particle phase, Atmos. Chem. Phys., 21, 12141-12153, 10.5194/acp-21-12141-2021, 2021.
Rogge, W. F., Hildemann, L. M., Mazurek, M. A., Cass, G. R., and Simoneit, B. R. T.: Sources of fine organic aerosol .4. Particulate abrasion products from leaf surfaces of urban plants, Environ. Sci. Technol., 27, 2700-2711, 10.1021/es00049a008, 1993.
Saleh, R., Hennigan, C. J., McMeeking, G. R., Chuang, W. K., Robinson, E. S., Coe, H., Donahue, N. M., and Robinson, A. L.: Absorptivity of brown carbon in fresh and photo-chemically aged biomass-burning emissions, Atmos. Chem. Phys., 13, 7683-7693, 10.5194/acp-13-7683-2013, 2013.
Saleh, R., Robinson, E. S., Tkacik, D. S., Ahern, A. T., Liu, S., Aiken, A. C., Sullivan, R. C., Presto, A. A., Dubey, M. K., Yokelson, R. J., Donahue, N. M., and Robinson, A. L.: Brownness of organics in aerosols from biomass burning linked to their black carbon content, Nat. Geosci., 7, 647-650, https://doi.org/10.1038/ngeo2220, 2014.



设置了格式: 字体颜色: 自动设置, 非突出显示
设置了格式: 字体颜色: 自动设置, 非突出显示
设置了格式: 字体颜色: 自动设置, 非突出显示
设置了格式: 字体颜色: 自动设置, 非突出显示
设置了格式: 字体颜色: 自动设置, 非突出显示
设置了格式: 字体颜色: 自动设置, 非突出显示
设置了格式: 字体颜色: 自动设置, 非突出显示
设置了格式: 字体颜色: 自动设置, 非突出显示
设置了格式: 字体颜色: 自动设置, 非突出显示
设置了格式: 字体颜色: 自动设置, 非突出显示
设置了格式: 非突出显示
设置了格式: 字体颜色: 自动设置, 非突出显示
设置了格式: 字体颜色: 自动设置
设置了格式: 字体颜色: 自动设置, 非突出显示

Saleh, R.: From measurements to models: Toward accurate representation of brown carbon in climate calculations, Curr. Pollut. Rep., 6, 90-104, 10.1007/s40726-020-00139-3, 2020.

Schauer, J. J., Mader, B. T., Deminter, J. T., Heidemann, G., Bae, M. S., Seinfeld, J. H., Flagan, R. C., Cary, R. A., Smith, D., Huebert, B. J., Bertram, T., Howell, S., Kline, J. T., Quinn, P., Bates, T., Turpin, B., Lim, H. J., Yu, J. Z., Yang, H., and Keywood, M. D.: ACE-Asia intercomparison of a thermal-optical method for the determination of particle-phase organic and elemental carbon, Environ. Sci. Technol., 37, 993-1001, 10.1021/es020622f, 2003.

Shetty, N. J., Pandey, A., Baker, S., Hao, W. M., and Chakrabarty, R. K.: Measuring light absorption by freshly emitted organic aerosols: Optical artifacts in traditional solvent-extraction-based methods, Atmos. Chem. Phys., 19, 8817-8830, 10.5194/acp-19-8817-2019, 2019.

Simoneit, B. R. T., and Fetzer, J. C.: High molecular weight polycyclic aromatic hydrocarbons in hydrothermal petroleums from the Gulf of California and Northeast Pacific Ocean, Org. Geochem., 24, 1065-1077, https://doi.org/10.1016/S0146-6380(96)00081-2, 1996.

Simoneit, B. R. T., Elias, V. O., Kobayashi, M., Kawamura, K., Rushdi, A. I., Medeiros, P. M., Rogge, W. F., and Didyk, B. M.: Sugars dominant water-soluble organic compounds in soils and characterization as tracers in atmospheric particulate matter, Environ. Sci. Technol., 38, 5939-5949, 10.1021/es0403099, 2004.

Song, C., Gyawali, M., Zaveri, R. A., Shilling, J. E., and Arnott, W. P.: Light absorption by secondary organic aerosol from α-pinene: Effects of oxidants, seed aerosol acidity, and relative humidity, J. Geophys. Res. Atmos., 118, 11,741-711,749, 10.1002/jgrd.50767, 2013.

Taylor, N. F., Collins, D. R., Lowenthal, D. H., McCubbin, I. B., Hallar, A. G., Samburova, V., Zielinska, B., Kumar, N., and Mazzoleni, L. R.: Hygroscopic growth of water soluble organic carbon isolated from atmospheric aerosol collected at US national parks and Storm Peak Laboratory, Atmos. Chem. Phys., 17, 2555-2571, 10.5194/acp-17-2555-2017, 2017.

Teich, M., van Pinxteren, D., Wang, M., Kecorius, S., Wang, Z., Müller, T., Močnik, G., and Herrmann, H.: Contributions of nitrated aromatic compounds to the light absorption of water-soluble and particulate brown carbon in different atmospheric environments in Germany and China, Atmos. Chem. Phys., 17, 1653-1672, 10.5194/acp-17-1653-2017, 2017.

Updyke, K. M., Nguyen, T. B., and Nizkorodov, S. A.: Formation of brown carbon via reactions of ammonia with secondary organic aerosols from biogenic and anthropogenic precursors, Atmos. Environ., 63, 22-31, https://doi.org/10.1016/j.atmosenv.2012.09.012, 2012.

Wang, X., Heald, C. L., Ridley, D. A., Schwarz, J. P., Spackman, J. R., Perring, A. E., Coe, H., Liu, D., and Clarke, A. D.: Exploiting simultaneous observational constraints on mass and absorption to estimate the global direct radiative forcing of black carbon and brown carbon, Atmos. Chem. Phys., 14, 10989-11010, 10.5194/acp-14-10989-2014, 2014.

Wang, X., Heald, C. L., Liu, J., Weber, R. J., Campuzano-Jost, P., Jimenez, J. L., Schwarz, J. P., and Perring, A. E.: Exploring the observational constraints on the simulation of brown carbon, Atmos. Chem. Phys., 18, 635-653, 10.5194/acp-18-635-2018, 2018.

Wang, Y., Hu, M., Wang, Y., Zheng, J., Shang, D., Yang, Y., Liu, Y., Li, X., Tang, R., Zhu, W., Du, Z., Wu, Y., Guo, S., Wu, Z., Lou, S., Hallquist, M., and Yu, J. Z.: The formation of nitro-aromatic compounds under high NOx and anthropogenic VOC conditions in urban Beijing, China, Atmos. Chem. Phys., 19, 7649-7665, 10.5194/acp-19-7649-2019, 2019.

Washenfelder, R. A., Attwood, A. R., Brock, C. A., Guo, H., Xu, L., Weber, R. J., Ng, N. L., Allen, H. M., Ayres, B. R., Baumann, K., Cohen, R. C., Draper, D. C., Duffey, K. C., Edgerton, E., Fry, J. L., Hu, W. W., Jimenez, J. L., Palm, B. B., Romer, P., Stone, E. A., Wooldridge, P. J., and Brown, S. S.: Biomass burning dominates brown carbon absorption in the rural southeastern United States, Geophys. Res. Lett., 42, 653-664, 10.1002/2014gl062444, 2015.

Weber, R. J., Sullivan, A. P., Peltier, R. E., Russell, A., Yan, B., Zheng, M., de Gouw, J., Warneke, C., Brock, C., Holloway, J. S., Atlas, E. L., and Edgerton, E.: A study of secondary organic aerosol formation in the anthropogenic-influenced southeastern United States, J. Geophys. Res. Atmos., 112, D13302, 10.1029/2007jd008408, 2007.

Xie, M., Chen, X., Hays, M. D., Lewandowski, M., Offenberg, J., Kleindienst, T. E., and Holder, A. L.: Light absorption of secondary organic aerosol: Composition and contribution of nitroaromatic compounds, Environ. Sci. Technol., 51, 11607-11616, 10.1021/acs.est.7b03263, 2017a.

Xie, M., Hays, M. D., and Holder, A. L.: Light-absorbing organic carbon from prescribed and laboratory biomass burning and gasoline vehicle emissions, Sci. Rep., 7, 7318, 10.1038/s41598-017-06981-8, 2017b.

Xie, M., Shen, G., Holder, A. L., Hays, M. D., and Jetter, J. J.: Light absorption of organic carbon emitted from burning wood, charcoal, and kerosene in household cookstoves, Environ. Pollut., 240, 60-67,

设置了格式: 字体颜色: 自动设置, 非突出显示

https://doi.org/10.1016/j.envpol.2018.04.085, 2018.
Xie, M., Chen, X., Hays, M. D., and Holder, A. L.: Composition and light absorption of N-containing aromatic compounds in organic aerosols from laboratory biomass burning, Atmos. Chem. Phys., 19, 2899-2915, 10.5194/acp-19-2899-2019, 2019a.
Xie, M., Chen, X., Holder, A. L., Hays, M. D., Lewandowski, M., Offenberg, J. H., Kleindienst, T. E., Jaoui, M., and Hannigan, M. P.: Light absorption of organic carbon and its sources at a southeastern U.S. location in summer, Environ. Pollut., 244, 38-46, https://doi.org/10.1016/j.envpol.2018.09.125, 2019b.
Xie, M., Zhao, Z., Holder, A. L., Hays, M. D., Chen, X., Shen, G., Jetter, J. J., Champion, W. M., and Wang, Q.: Chemical composition, structures, and light absorption of N-containing aromatic compounds emitted from burning wood and charcoal in household cookstoves, Atmos. Chem. Phys., 20, 14077-14090, 10.5194/acp-20-14077-2020, 2020.
Xie, M., Peng, X., Shang, Y., Yang, L., Zhang, Y., Wang, Y., and Liao, H.: Collocated ~~Measurements~~ measurements of Light-absorbing organic carbon in PM2.5: Observation uncertainty and organic tracer-based source apportionment, J. Geophys. Res. Atmos., 127, e2021JD035874, https://doi.org/10.1029/2021JD035874, 2022.
Xu, Z., Feng, W., Wang, Y., Ye, H., Wang, Y., Liao, H., and Xie, M.: Replication Data for: Underestimation of brown carbon absorption based on the methanol extraction method and its impacts on source analysis, Harvard Dataverse, ~~V1~~V2, https://doi.org/10.7910/DVN/CGHPXB~~https://doi.org/10.7910/DVN/CGHPXB~~, 2022.
Xu, L., Peng, Y., Ram, K., Zhang, Y., Bao, M., and Wei, J.: Investigation of the uncertainties of simulated optical properties of brown carbon at two Asian sites using a modified bulk aerosol optical scheme of the community atmospheric model version 5.3, J. Geophys. Res. Atmos., 126, e2020JD033942, https://doi.org/10.1029/2020JD033942, 2021.
Yan, F., Kang, S., Sillanpää, M., Hu, Z., Gao, S., Chen, P., Gautam, S., Reinikainen, S.-P., and Li, C.: A new method for extraction of methanol-soluble brown carbon: Implications for investigation of its light absorption ability, Environ. Pollut., 262, 114300, https://doi.org/10.1016/j.envpol.2020.114300, 2020.
Yang, L., Shang, Y., Hannigan, M. P., Zhu, R., Wang, Q. g., Qin, C., and Xie, M.: Collocated speciation of PM2.5 using tandem quartz filters in northern nanjing, China: Sampling artifacts and measurement uncertainty, Atmos. Environ., 246, 118066, https://doi.org/10.1016/j.atmosenv.2020.118066, 2021.
Yu, Y., Ding, F., Mu, Y., Xie, M., and Wang, Q. g.: High time-resolved PM2.5 composition and sources at an urban site in Yangtze River Delta, China after the implementation of the APPCAP, Chemosphere, 261, 127746, https://doi.org/10.1016/j.chemosphere.2020.127746, 2020.
Zhang, A., Wang, Y., Zhang, Y., Weber, R. J., Song, Y., Ke, Z., and Zou, Y.: Modeling the global radiative effect of brown carbon: a potentially larger heating source in the tropical free troposphere than black carbon, Atmos. Chem. Phys., 20, 1901-1920, 10.5194/acp-20-1901-2020, 2020.
Zhang, X., Hecobian, A., Zheng, M., Frank, N. H., and Weber, R. J.: Biomass burning impact on PM2.5 over the southeastern US during 2007: integrating chemically speciated FRM filter measurements, MODIS fire counts and PMF analysis, Atmos. Chem. Phys., 10, 6839-6853, 10.5194/acp-10-6839-2010, 2010.
Zhang, X., Lin, Y.-H., Surratt, J. D., and Weber, R. J.: Sources, composition and absorption Ångström exponent of light-absorbing organic components in aerosol extracts from the Los Angeles basin, Environ. Sci. Technol., 47, 3685-3693, 10.1021/es305047b, 2013.
Zhu, C.-S., Cao, J.-J., Huang, R.-J., Shen, Z.-X., Wang, Q.-Y., and Zhang, N.-N.: Light absorption properties of brown carbon over the southeastern Tibetan Plateau, Sci. Total Environ., 625, 246-251, https://doi.org/10.1016/j.scitotenv.2017.12.183, 2018.

**设置了格式:** 字体颜色: 自动设置, 非突出显示

**设置了格式:** 非突出显示

Table 1. SEOC concentrations and extraction efficiencies (η, %) of total OC and OC fractions for different solvents.

| | OC prior to extractions | Water[a] | MeOH[b] | MeOH/DCM (1:1)[b] | MeOH/DCM (1:2)[b] | THF[b] | DMF[a] |
|---|---|---|---|---|---|---|---|
| **One-time extraction (*N* = 11)** | | | | | | | |
| *SEOC, μg m$^{-3}$* | | | | | | | |
| Total OC | 9.36 ± 2.27 | 6.38 ± 2.03 | 7.85 ± 2.40 | 7.08 ± 1.32 | 6.99 ± 1.71 | 6.14 ± 2.01 | 8.49 ± 2.52 |
| OC1 | 0.66 ± 0.21 | 0.61 ± 0.20 | 0.64 ± 0.21 | 0.65 ± 0.20 | 0.64 ± 0.22 | 0.59 ± 0.18 | 0.59 ± 0.24 |
| OC2 | 2.69 ± 0.55 | 2.20 ± 0.60 | 2.50 ± 0.55 | 2.34 ± 0.41 | 2.37 ± 0.46 | 2.09 ± 0.55 | 2.48 ± 0.60 |
| OC3 | 3.35 ± 0.93 | 1.82 ± 0.80 | 2.48 ± 0.96 | 2.23 ± 0.49 | 2.18 ± 0.70 | 1.98 ± 0.93 | 2.86 ± 1.01 |
| OC4 | 2.75 ± 0.81 | 1.76 ± 0.65 | 2.23 ± 0.84 | 1.86 ± 0.51 | 1.78 ± 0.61 | 1.48 ± 0.61 | 2.56 ± 0.87 |
| *η (%)* | | | | | | | |
| Total OC | | 66.7 ± 8.58 | 82.3 ± 8.68 | 76.0 ± 7.70 | 74.3 ± 7.83 | 64.2 ± 8.08 | 89.0 ± 7.96 |
| OC1 | | 91.7 ± 4.85 | 96.1 ± 6.73 | 97.9 ± 5.02 | 97.4 ± 4.35 | 89.6 ± 9.55 | 88.8 ± 4.98 |
| OC2 | | 80.8 ± 8.11 | 92.7 ± 3.69 | 87.7 ± 5.87 | 88.5 ± 7.21 | 76.9 ± 7.62 | 91.4 ± 6.17 |
| OC3 | | 52.4 ± 11.8 | 73.0 ± 11.5 | 68.1 ± 8.64 | 65.2 ± 10.2 | 57.6 ± 12.0 | 84.3 ± 9.79 |
| OC4 | | 63.3 ± 9.13 | 80.3 ± 11.4 | 69.0 ± 9.26 | 64.5 ± 8.11 | 52.7 ± 5.86 | 92.8 ± 9.69 |
| **Two-time extraction (*N* = 10)** | | | | | | | |
| *SEOC, μg m$^{-3}$* | | | | | | | |
| Total OC | 10.9 ± 4.93 | 7.74 ± 4.01 | 9.33 ± 4.11 | 9.34 ± 4.19 | 9.11 ± 4.04 | 7.56 ± 3.38 | 10.4 ± 4.80 |
| OC1 | 0.66 ± 0.47 | 0.62 ± 0.45 | 0.62 ± 0.49 | 0.59 ± 0.50 | 0.60 ± 0.51 | 0.59 ± 0.49 | 0.60 ± 0.47 |
| OC2 | 2.76 ± 0.77 | 2.20 ± 0.59 | 2.60 ± 0.66 | 2.57 ± 0.65 | 2.60 ± 0.68 | 2.28 ± 0.53 | 2.69 ± 0.78 |
| OC3 | 4.11 ± 2.01 | 2.55 ± 1.62 | 3.26 ± 1.62 | 3.37 ± 1.68 | 3.20 ± 1.58 | 2.62 ± 1.39 | 3.88 ± 1.95 |
| OC4 | 3.36 ± 1.77 | 2.38 ± 1.42 | 2.84 ± 1.42 | 2.81 ± 1.47 | 2.71 ± 1.39 | 2.08 ± 1.06 | 3.23 ± 1.70 |
| *η (%)* | | | | | | | |
| Total OC | | 69.9 ± 5.88 | 86.6 ± 7.86 | 86.2 ± 8.73 | 84.8 ± 7.76 | 70.1 ± 8.01 | 95.6 ± 3.67 |
| OC1 | | 93.6 ± 4.08 | 90.3 ± 13.9 | 82.6 ± 25.9 | 83.8 ± 22.4 | 82.9 ± 15.1 | 92.2 ± 13.9 |
| OC2 | | 80.1 ± 5.01 | 94.8 ± 4.20 | 93.6 ± 4.94 | 94.7 ± 2.51 | 83.5 ± 6.86 | 97.2 ± 2.12 |
| OC3 | | 59.0 ± 10.6 | 80.0 ± 10.2 | 82.3 ± 9.86 | 79.1 ± 10.6 | 63.9 ± 10.7 | 94.2 ± 4.15 |
| OC4 | | 69.3 ± 6.46 | 86.3 ± 12.0 | 84.3 ± 12.0 | 82.7 ± 13.3 | 62.9 ± 7.76 | 96.9 ± 5.18 |

[a] Concentrations of rOC in extracted filters were measured after the baking process (100 °C, 2 h); [b] rOC was measured when extracted filters were air dried.

设置了格式: 字体: 小四

Table 2. Light-absorbing properties of SEOC following one-time and two-time extraction procedures.

设置了格式: 字体: 小四

带格式的: 缩进: 左 -4.73 字符, 首行缩进: 0 字符

| Solvent | Water | MeOH | MeOH/DCM (1:1) | MeOH/DCM (1:2) | THF | DMF |
|---|---|---|---|---|---|---|
| **One-time extraction** | | | | | | |
| $Abs_{365}$, $Mm^{-1}$ | 5.13 ± 2.04 | 11.9 ± 5.83 | 10.3 ± 4.42 | 8.12 ± 3.38 | 5.48 ± 3.01 | 17.5 ± 8.05 |
| $Abs_{550}$, $Mm^{-1}$ | 0.35 ± 0.12 | 1.28 ± 0.87 | 0.97 ± 0.55 | 0.35 ± 0.47 | 0.42 ± 0.47 | 4.40 ± 2.34 |
| $MAE_{365}$, $m^2\ g^{-1}$ C | 0.87 ± 0.19 | 1.46 ± 0.41 | 1.41 ± 0.36 | 1.13 ± 0.22 | 0.87 ± 0.25 | 2.02 ± 0.58 |
| $MAE_{550}$, $m^2\ g^{-1}$ C | 0.062 ± 0.028 | 0.15 ± 0.084 | 0.13 ± 0.054 | 0.042 ± 0.52 | 0.059 ± 0.56 | 0.30 ± 0.12 |
| Å | 6.63 ± 0.49 | 5.44 ± 0.75 | 5.65 ± 0.54 | 6.59 ± 0.66 | 6.17 ± 0.69 | 4.52 ± 0.41 |
| **Two-time extraction** | | | | | | |
| $Abs_{365,1st}$,[a] $Mm^{-1}$ | 6.64 ± 4.25 | 14.1 ± 7.09 | 14.6 ± 8.05 | 11.6 ± 6.78 | 7.17 ± 4.26 | 20.5 ± 10.6 |
| $Abs_{550,1st}$,[a] $Mm^{-1}$ | 0.42 ± 0.12 | 1.34 ± 0.70 | 1.34 ± 0.83 | 0.84 ± 0.50 | 0.53 ± 0.27 | 2.82 ± 1.44 |
| $Abs_{365}$,[b] $Mm^{-1}$ | 8.26 ± 5.21 | 15.5 ± 7.76 | 16.8 ± 8.82 | 14.0 ± 8.91 | 8.35 ± 4.81 | 21.9 ± 11.2 |
| $Abs_{550}$,[b] $Mm^{-1}$ | 0.50 ± 0.18 | 1.60 ± 0.78 | 1.64 ± 0.99 | 1.22 ± 0.98 | 0.69 ± 0.43 | 3.01 ± 1.49 |
| $MAE_{365}$, $m^2\ g^{-1}$ C | 1.19 ± 0.26 | 1.70 ± 0.60 | 1.80 ± 0.52 | 1.50 ± 0.51 | 1.10 ± 0.40 | 2.11 ± 0.49 |
| $MAE_{550}$, $m^2\ g^{-1}$ C | 0.082 ± 0.30 | 0.19 ± 0.11 | 0.17 ± 0.083 | 0.13 ± 0.069 | 0.094 ± 0.054 | 0.29 ± 0.075 |
| Å | 6.32 ± 0.58 | 5.37 ± 0.57 | 5.47 ± 0.67 | 5.57 ± 0.39 | 6.06 ± 0.54 | 4.53 ± 0.21 |

[a] Light absorption coefficient of SEOC after the first extraction; [b] sum of SEOC absorption in 1st and 2nd extracts.

Table 3. Comparisons of light-absorbing properties of ambient $PM_{2.5}$ extracts in DMF and MeOH derived from duplicate $Q_f$–$Q_b$ data ($N$ = 109).

| | DMF | | | MeOH[a] | | |
|---|---|---|---|---|---|---|
| | Median | Mean ± std | Range | Median | Mean ± std | Range |
| $Abs_{365}$, $Mm^{-1}$ | 6.99 | 8.42 ± 5.40 | 1.14–30.8 | 5.59 | 6.43 ± 4.66 | 0.38–29.6 |
| $MAE_{365}$, $m^2\ g^{-1}C$ | 1.13 | 1.20 ± 0.49 | 0.34–2.45 | 0.91 | 1.03 ± 0.58 | 0.089–2.49 |
| Å | 5.21 | 5.25 ± 0.64 | 3.21–6.82 | 6.49 | 6.81 ± 1.64 | 4.34–11.3 |

[a] Data for MeOH extracts were obtained from Xie et al. (2022).

设置了格式: 字体: 小四

设置了格式: 上标

Figure 1

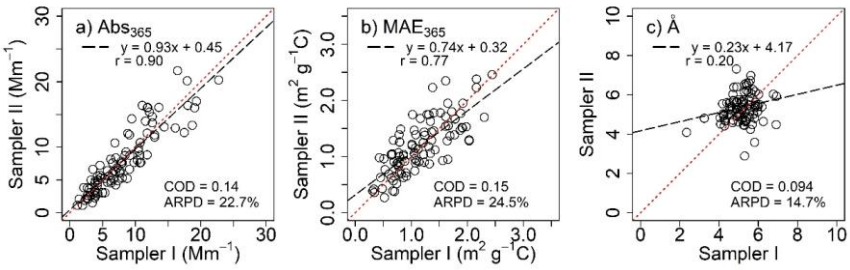


Figure 1. Comparisons between collocated measurements for light-absorbing properties of $PM_{2.5}$ extracts in DMF after $Q_b$ corrections.

设置了格式: 字体: 小四

Figure 2

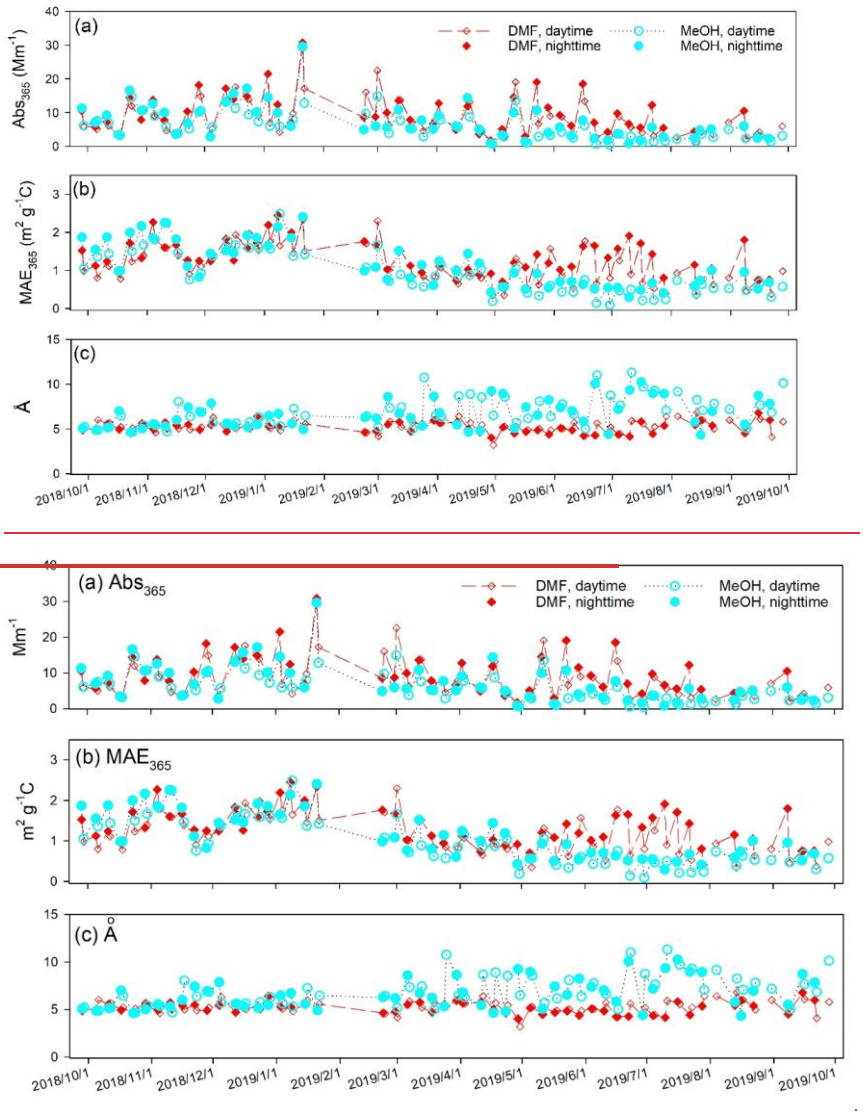





Figure 2. Time series comparisons of light-absorbing properties of DMF and MeOH extracts using artifact-corrected data. MeOH extract data were obtained from Xie et al. (2022).

设置了格式: 字体: 小四

Figure 3

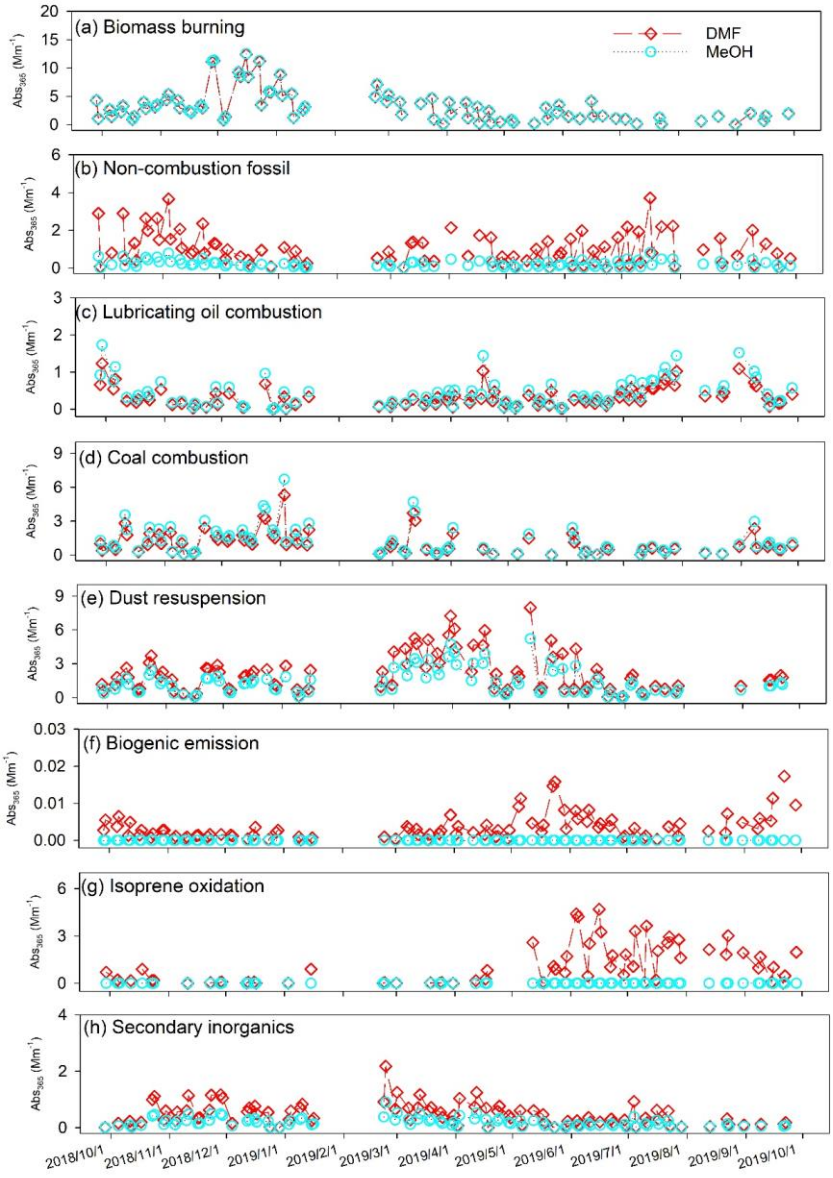
(a) Biomass burning
DMF
MeOH
(b) Non-combustion fossil
(c) Lubricating oil combustion
(d) Coal combustion
(e) Dust resuspension
(f) Biogenic emission
(g) Isoprene oxidation
(h) Secondary inorganics
Abs365 (Mm-1)
2018/10/1
2018/11/1
2018/12/1
2019/1/1
2019/2/1
2019/3/1
2019/4/1
2019/5/1
2019/6/1
2019/7/1
2019/8/1
2019/9/1
2019/10/1

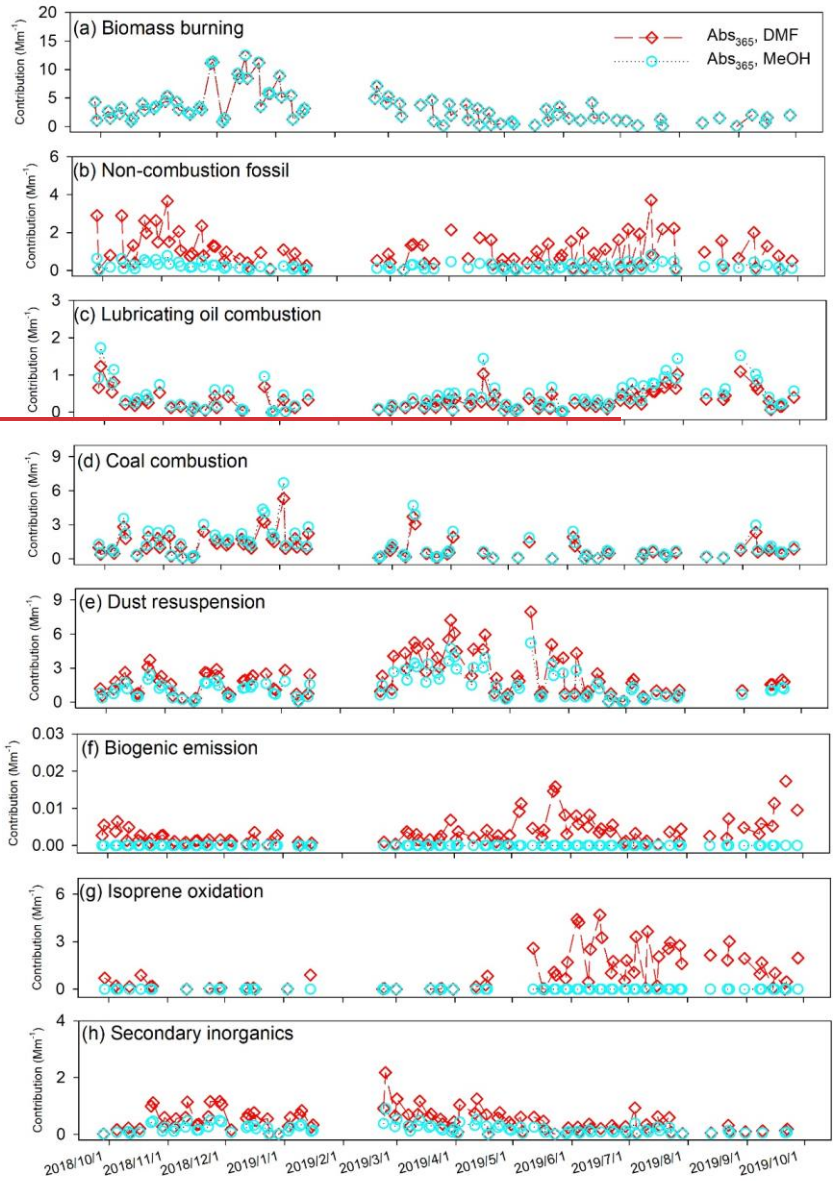


Figure 3. Time series of factor contributions to $Abs_{365}$ of DMF and MeOH extracts of ambient $PM_{2.5}$ samples.

设置了格式: 字体: 小四